HHS Public Access

Author manuscript

Immunology. Author manuscript; available in PMC 2022 September 01.

Published in final edited form as:

Immunology. 2022 September ; 167(1): 105–121. doi:10.1111/imm.13527.

Keap1 moderates the transcription of virus induced genes through G9a-GLP and NFκB p50 recruitment

Veronica Elizabeth Burns,

Tom Klaus Kerppola[#]

Department of Biological Chemistry, University of Michigan, Ann Arbor, MI 48109-5606

Abstract

Cells must control genes that are induced by virus infection to mitigate deleterious consequences of inflammation. We investigated the mechanisms whereby Keap1 moderates the transcription of genes that are induced by Sendai virus infection in mouse embryo fibroblasts (MEFs). *Keap1−/−* deletions increased the transcription of virus induced genes independently of Nrf2. Keap1 moderated early virus induced gene transcription. Virus infection induced Keap1 to bind *Ifnb1*, *Tnf* and *Il6,* and reduced Keap1 binding at *Cdkn1a* and *Ccng1*. Virus infection induced G9a-GLP and NFκB p50 recruitment, and H3K9me2 deposition. *Keap1−/−* deletions eliminated G9a-GLP and NFκB p50 recruitment, and H3K9me2 deposition, but they did not affect NFκB p65, IRF3 or cJun recruitment. G9a-GLP inhibitors (BIX01294, MS012, BRD4770) enhanced virus induced gene transcription in MEFs with intact *Keap1*, but not in MEFs with *Keap1−/−* deletions. G9a-GLP inhibitors augmented Keap1 binding to virus induced genes in infected MEFs, and to cell cycle genes in uninfected MEFs. G9a-GLP inhibitors augmented NFκB subunit recruitment in MEFs with intact *Keap1.* G9a-GLP inhibitors stabilized Keap1 retention in permeabilized MEFs. G9a-GLP lysine methyltransferase activity was required for Keap1 to moderate transcription, and it moderated Keap1 binding to chromatin. The interdependent effects of Keap1 and G9a-GLP on the recruitment of each other and on the moderation of virus induced gene transcription constitute a feedback circuit. Keap1 and the electrophile tBHQ reduced virus induced gene transcription through different mechanisms, and they regulated the recruitment of different NFκB subunits. Characterization of the mechanisms whereby Keap1, G9a-GLP and NFκB p50 moderate virus induced gene transcription can facilitate the development of immunomodulatory agents.

Graphical Abstract

[#]Address correspondence to Tom Kerppola, kerppola@umich.edu.

Author contributions: TKK conceived the study. VEB and TKK designed the experiments. VEB performed the experiments. TKK and VEB analyzed the data and wrote the paper.

Declaration of interests: The authors declare that competing interests did not influence the design or the interpretation of the experiments.

Ethics approval and consent to participate: All experiments with live mice were approved by the Institutional Animal Care & Use Committee at University of Michigan.

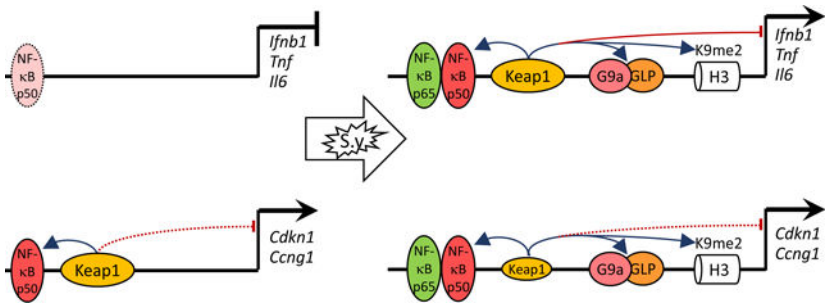

Excess and maladaptive immune responses to virus infections are a major contributing factor to the morbidity and mortality of COVID-19 and other diseases. Conversely, inadequate immune responses to vaccines and pathogens by individuals with suppressed immune function expose them to infections. Burns and Kerppola characterize molecular mechanisms that moderate the transcription of genes that are induced by virus infection. Characterization of the mechanisms whereby Keap1, G9a-GLP and NFκB p50 moderate virus induced gene transcription identifies new targets for therapeutic agents that can modulate immune responsiveness.

Keywords

Sendai virus induced gene transcription; moderation of transcription; virus induced chromatin modification; lysine methyltransferase recruitment; stability of chromatin binding; sentinel cell gene regulation

Introduction

Virus infection induces the transcription of innate immune response genes. Excess virus induced gene transcription has deleterious effects. Elucidation of the factors and molecular mechanisms that moderate the transcription of virus induced genes is necessary to understand how homeostasis is maintained during viral infections.

Keap1 (Kelch-like ECH-associated protein) deletion in the mouse germline causes inflammatory cell infiltration of the gastric mucosa and kidneys (1, 2). Conditional Keap1 deletion in Tregs causes lung and liver inflammation (3). Conversely, conditional *Keap1* deletions in Clara cells, macrophages, thymocytes, and renal tubule cells reduce experimentally induced inflammatory responses (4–7). The pro- and anti-inflammatory effects of *Keap1* deletions suggest that Keap1 influences immune functions through multiple mechanisms.

Keap1 depletion can enhance or reduce the induction of cytokine transcription in cultured cells. Keap1 depletion in human primary monocyte derived macrophages and in macrophage cell lines enhances cytokine induction by *Mycobacterium avium* infection and by LPS, respectively (8, 9). Conversely, *Keap1* deletion in mouse bone marrow derived macrophages reduces cytokine induction by LPS and IFNγ (10). The contrasting effects of Keap1 depletions on cytokine induction could be due to indirect effects of Keap1 depletion on different factors that influence cytokine transcription in different macrophages (8–10).

Fibroblasts respond rapidly to virus infection and serve as sentinel cells of the immune system (11). Lymphocytic choriomeningitis virus infection in mice induces immune response genes in the fibroblasts of many organs (12). Influenza virus infection in mice induces changes in lung fibroblast gene expression in regions of interstitial inflammation (13). Mouse embryo fibroblasts (MEFs) can be used to study mechanisms of gene regulation in naïve cells that have not been exposed to immune stimuli.

We found that Keap1 reduces the levels of cytokine transcripts that are induced by Sendai virus infection in mouse embryo fibroblasts (MEFs) (14). Virus infection induces Keap1 binding to cytokine genes. Keap1 is required for G9a (*Ehmt2*) and GLP (*Ehmt1*) lysine methyltransferase recruitment to virus induced genes. G9a and GLP catalyze histone H3 lysine 9 dimethylation (H3K9me2) in euchromatin, and they have overlapping and interdependent activities (15, 16). G9a and GLP are associated with the repression of cytokine transcription (17–19). They are required for the differentiation and functions of both innate and adaptive immune cells (20–22).

Keap1 is also required for NFκB p50 recruitment to virus induced genes (14). NFκB p50 can both repress and activate cytokine transcription, whereas NFκB p65 activates transcription. NFκB p50 deficiency causes immune dysfunctions in mice and in human patients (23–25). Chromatin binding by Keap1 complexes with NFκB p50 and NFκB p65 was visualized using BiFC analysis (14). Keap1 also binds to specific genomic loci on Drosophila polytene chromosomes (26, 27).

To elucidate the mechanisms whereby Keap1 moderates virus induced gene transcription, we examined the relationships among Keap1, G9a-GLP and NFκB recruitment. We investigated the roles of G9a-GLP lysine methyltransferase activity in the moderation of virus induced gene transcription by Keap1, and in Keap1 binding to chromatin. We analyzed the relationships between the moderation of transcription by Keap1 and the effects of electrophiles on cytokine induction.

Materials and Methods

MEF derivation and virus infection.

Mice with *Keap1* and *Nrf2* deletions (1, 28) were crossed to generate *Keap1−/+ Nrf2−/+* heterozygous mice. Primary MEFs were isolated at about 13 days post coitus from embryos that were produced by these mice. MEFs from different embryos are identified in the figures and figure legends by #number after the genotype. The MEFs were expanded for up to 5 passages and the compounds indicated or vehicle were added to the cultures. The MEFs were infected by the addition of 200 HA units/ml Sendai virus (Charles River Laboratories, Wilmington, MA).

Transcript quantification and ChIP analyses.

RNA was isolated at the times indicated, reverse transcribed and quantified by qPCR. Crosslinked chromatin was prepared, fragmented, precipitated using the antibodies indicated, decrosslinked, and quantified by qPCR. The reproducibility of the findings

was evaluated in different sets of MEFs by ANOVA analyses and multiple testing was compensated as described by Šidák.

Analyses of protein retention in MEFs.

The stabilities of protein retention in MEFs were evaluated by incubating the MEFs in buffers containing the indicated detergents followed by separation of the retained and released proteins by centrifugation and quantification by western blot analyses. After culture with or without G9a-GLP inhibitors, the MEFs were incubated in buffers containing detergents that disrupt protein interactions. The proteins that were released and retained were analyzed by immunoblotting.

Please see supplementary information for detailed descriptions of materials and methods that are not unique to this study. These include mouse husbandry, MEF culture and infection, transcript isolation and analysis, chromatin isolation and analysis, analysis of protein retention in MEFs, immunoblotting, sources and use of G9a-GLP inhibitors, sources of antibodies and chemicals, oligonucleotide sequences, and statistical methods and software.

Results

We investigated Keap1 functions at genes whose transcription was induced by Sendai virus infection and at uninduced genes. We compared the transcript levels in virus infected and in uninfected MEFs with intact *Keap1* and with *Keap1−/−* deletions (Figure 1). To avoid the indirect effects of *Keap1−/−* deletions that result from constitutive Nrf2 activation, we focused on the effects of *Keap1−/−* deletions in MEFs that also carried *Nrf2−/−* deletions (*Keap1−/− Nrf2−/−* MEFs). We measured the transcript levels at different times after virus infection to characterize the effects of Keap1 on the primary transcriptional response.

Virus infection induced *Ifnb1*, *Tnf* and *Il6* transcription more rapidly and to higher levels in *Keap1−/− Nrf2−/−* MEFs than in MEFs with intact *Keap1* (Figure 1A). The higher transcript levels were observed at the earliest time examined 2 h after virus infection. The peak *Ifnb1*, *Tnf* and *Il6* transcript levels were 3- to 8-fold higher on average in 7 different sets of *Keap1−/− Nrf2−/−* MEFs relative to MEFs with intact *Keap1*. Keap1 reduced the levels of virus induced transcripts in the absence of Nrf2, indicating that Keap1 moderated virus induced gene transcription independently of Nrf2 (Figure 1A, S1).

We also examined Keap1 effects on cell cycle associated gene transcription. Virus infection induced *Cdkn1a* transcription in two of the three different *Keap1−/− Nrf2−/−* MEFs that were tested (Figure 1A, Figure 3B). In contrast, virus infection did not induce *Cdkn1a* transcription in any of the three MEFs with intact *Keap1*. The basal levels of *Cdkn1a* and *Ccng1* transcripts were higher in *Keap1−/− Nrf2−/−* MEFs than in MEFs with intact *Keap1* (Figure 1A, Figure 3B). Keap1 suppressed latent viral induction of *Cdkn1a* transcription.

There was no significant difference in the levels of *Gapdh*, *Nqo1,* or Sendai virus M gene transcripts between *Keap1−/− Nrf2−/−* MEFs and MEFs with intact *Keap1* at early times after virus infection (Figure 1A, Figure 2A). Keap1 did not affect the efficiencies of virus infection or replication, or the transcription of these genes.

Virus infection induces Keap1 recruitment to cytokine genes, and reduces Keap1 binding at cell cycle genes

We evaluated the specificity of Keap1 recruitment to different genes upon virus infection by comparing the effects of virus infection on Keap1 binding to the promoter regions of cytokine and cell cycle associated genes. Virus infection induced Keap1 to bind *Ifnb1*, *Tnf* and *Il6* in the 7 different MEFs with intact *Keap1* that were tested (Figure 1B, 1C). The αKeap1 ChIP signals at these genes were 11- to 14-fold higher, on average, in virus infected MEFs than in uninfected MEFs. We established that the ChIP signals reflected Keap1 binding to virus induced genes by using antibodies that recognized different epitopes in Keap1 and by employing several independent criteria to establish the validity of the ChIP signals (Figure S2). Since Keap1 bound to these genes upon virus infection, and since the levels of these transcripts were higher in *Keap1−/− Nrf2−/−* MEFs than in MEFs with intact *Keap1*, we inferred that Keap1 moderated their transcription by binding to the genes upon virus infection.

Keap1 bound to *Cdkn1a* and *Ccng1* in uninfected MEFs. Virus infection reduced Keap1 binding to these genes in the 4 different MEFs that were tested (Figure 1B, 1C). The average αKeap1 ChIP signals at *Cdkn1a* and *Ccng1* were 21% and 23% lower, respectively, in virus infected MEFs than in uninfected MEFs. The differences in the effects of virus infection on Keap1 binding to *Ifnb1*, *Tnf* and *Il6* versus *Cdkn1a* and *Ccng1* suggest that virus infection regulated Keap1 binding to different genes by selective mechanisms.

Keap1 is required for G9a and GLP recruitment and for H3K9me2 deposition induced by virus infection

We examined the relationships among Keap1, G9a and GLP recruitment, and H3K9me deposition by comparing them at different genes in virus infected and in uninfected MEFs, and in MEFs with intact *Keap1* and in MEFs with *Keap1−/−* deletions. Virus infection induced G9a and GLP to bind *Ifnb1*, *Tnf* and *Il6* in the 3 different MEFs with intact *Keap1* that were tested (Figure 1B). Virus infection also induced G9a and GLP to bind *Cdkn1a* and *Ccng1*, and 10 kb upstream of *Ifnb1* in MEFs with intact *Keap1*. Virus infection did not induce G9a or GLP to bind the genes that were examined in *Keap1−/− Nrf2−/−* MEFs. The αG9a and αGLP ChIP signals at these genes were 3- to 7-fold higher on average in virus infected MEFs with intact *Keap1* than in *Keap1−/− Nrf2−/−* MEFs. Since Keap1 was required for both G9a and GLP recruitment, and since both G9a and GLP have lysine methyltransferase activity and can form heterodimers, we refer to these complexes collectively as G9a-GLP. Keap1 expression was required for G9a-GLP recruitment both to virus induced genes and to cell cycle genes in virus infected MEFs.

We examined the effects of virus infection on H3K9me2 deposition in MEFs with intact *Keap1* and in MEFs with *Keap1−/−* deletions. Virus infection induced H3K9me2 deposition at all genes that were examined in the 6 different MEFs with intact *Keap1* that were tested (Figure 1B). By contrast, virus infection did not increase H3K9me2 deposition at any of the genes tested in *Keap1−/− Nrf2−/−* MEFs. *Keap1−/−* deletions did not affect the basal H3K9me2 levels in uninfected MEFs. It is likely that the lack of virus induced H3K9me2

deposition in *Keap1−/− Nrf2−/−* MEFs was due to the lack of virus induced G9a or GLP recruitment in these MEFs.

Virus infection induced G9a-GLP recruitment and H3K9me2 deposition in flanking regions upstream and downstream of the *Ifnb1* gene. Virus infection did not increase the H3K9me1 level or the total H3 ChIP signal in the regions that were tested (Figure S3). The H3K9me2 ChIP signals at virus induced genes were higher than the H3K9me2 signals at major satellite repeats, but they were lower than the H3K9me2 ChIP signals at telomere repeats (Figure S3). These relative H3K9me2 levels were observed whether the ChIP signals were normalized by the H3K9me1 or total H3 ChIP signals in these regions. Virus infection reduced H3K27me3 at the genes that were tested both in *Keap1−/− Nrf2−/−* MEFs and in MEFs with intact *Keap1* (Figure 3A). Keap1 was required for virus induced H3K9me2 deposition selectively.

Keap1 as well as virus infection have distinct effects on NFκB p50 *versus* NFκB p65 recruitment

We examined the relationships between Keap1 and NFκB subunit recruitment by comparing binding by different NFκB subunits at virus induced and uninduced genes in MEFs with intact *Keap1*, and in MEFs with *Keap1−/−* deletions. Virus infection induced NFκB p50 to bind *Ifnb1* in the 6 different MEFs with intact *Keap1* that were tested (Figure 1C). Virus infection did not induce NFκB p50 to bind *Ifnb1* in the 5 different *Keap1−/− Nrf2−/−* MEFs that were tested. Keap1 was necessary for NFκB p50 recruitment to *Ifnb1*, and Keap1 and NFκB p50 binding to *Ifnb1* were correlated in different virus infected MEFs with intact *Keap1*.

NFκB p50 binding to *Tnf* was detected upon virus infection in about half of the experiments (Figure 1C, Figure 2B, Figure 3A, Figure 6B). Virus infection induced NFκB p50 to bind *Tnf* in at least one experiment with each of the 6 different MEFs with intact *Keap1*. Virus infection did not induce NFκB p50 to bind *Tnf* in any experiments with the 5 different *Keap1−/− Nrf2−/−* MEFs.

NFκB p50 bound to *Il6* in 2 of the 6 uninfected MEFs with intact *Keap1*, and in all 6 virus infected MEFs with intact *Keap1* (Figure 1C, Figure 2B, Figure 3A). NFκB p50 did not bind to *Il6* in the 5 different *Keap1−/− Nrf2−/−* MEFs in the absence or in the presence of virus. Consequently, *Keap1* was required for virus induced NFκB p50 recruitment to *Ifnb1*, *Tnf* and *Il6*.

NFκB p50 bound to *Cdkn1a* and *Ccng1* in the absence of virus infection in the 5 different MEFs with intact *Keap1* that were tested (Figure 1C, Figure 2B, Figure 3A). Virus infection augmented NFκB p50 binding to *Cdkn1a* and *Ccng1* in MEFs with intact *Keap1*. NFκB p50 did not bind to *Cdkn1a* or *Ccng1* in *Keap1−/− Nrf2−/−* MEFs in the absence or in the presence of virus. *Keap1* was required for NFκB p50 to bind *Cdkn1a* and *Ccng1* in virus infected and in uninfected MEFs.

NFκB p65 bound to *Cdkn1a* and *Ccng1* only in virus infected MEFs, whereas NFκB p50 bound to these genes also in uninfected MEFs (Figure 1C, Figure 2B). Virus infection

induced NFκB p65 binding to all the genes tested in *Keap1−/− Nrf2−/−* MEFs, whereas virus infection induced little or no NFκB p50 binding to these genes in *Keap1−/− Nrf2−/−* MEFs. Thus, *Keap1* was required for NFκB p50 binding, but virus infection was not. In contrast, *Keap1* was not required for NFκB p65 binding, but little binding was detected in uninfected MEFs.

Virus infection induced equivalent levels of IRF3 as well as cJun binding in *Keap1−/− Nrf2−/−* MEFs and in MEFs with intact *Keap1* at the genes that were examined (Figure 1B, 1C). Keap1 was required for G9a-GLP and NFκB p50 recruitment selectively.

G9a-GLP inhibition enhances the transcription of virus induced genes in MEFs with intact *Keap1* selectively

We examined if G9a-GLP lysine methyltransferase activity was required for Keap1 moderation of virus induced gene transcription by comparing the effects of G9a-GLP inhibitors on transcription in MEFs with intact *Keap1* and in MEFs with *Keap1−/−* deletions. BIX01294 binds to the peptide binding groove of G9a and inhibits its lysine methyltransferase activity (29, 30). BIX01294 was added to the MEFs one hour before virus infection to focus on the direct effects of G9a-GLP inhibition. BIX01294 enhanced *Ifnb1*, *Tnf*, and *Il6* transcription in the 4 different MEFs with intact *Keap1* that were tested (Figure 2A, left column). The peak *Ifnb1*, *Tnf* and *Il6* transcript levels were 2.3- to 2.4-fold higher on average in the MEFs with intact *Keap1* that were cultured with BIX01294 than in the same MEFs that were cultured with vehicle. In contrast, BIX01294 did not increase the peak *Ifnb1*, *Tnf*, or *Il6* transcript levels in *Keap1−/− Nrf2−/−* MEFs (Figure 2A, right column). BIX01294 increased *Ifnb1* and *Il6* transcript levels by the same amount as *Keap1−/−* deletions. Since Keap1 moderated the transcription of virus induced genes, and since BIX01294 enhanced the transcription of virus induced genes selectively in MEFs with intact *Keap1*, we inferred that BIX01294 counteracted the ability of Keap1 to moderate the transcription of virus induced genes.

BIX01294 did not increase *Gapdh*, *Cdkn1a, Ccng1* or viral M gene transcript levels within 6 h after virus infection (Figure 2A, Figure 3B). BIX01294 enhanced virus induced gene transcription in MEFs with intact *Keap1* rapidly and selectively.

G9a-GLP inhibition augments Keap1 binding to different genes in virus infected versus uninfected MEFs

We analyzed the specificity of BIX01294 effects on Keap1 binding by comparing its effects on Keap1 binding to virus induced and to uninduced genes in virus infected and in uninfected MEFs. BIX01294 augmented Keap1 binding to *Ifnb1*, *Tnf* and *Il6* upon virus infection in the 5 different MEFs with intact *Keap1* that were tested (Figure 2B, Figure 3B). The αKeap1 ChIP signals at these genes were 1.9- to 2.1-fold higher, on average, in virus infected MEFs that were cultured with BIX01294 than in the same MEFs that were cultured with vehicle.

BIX01294 augmented Keap1 binding to *Cdkn1a* and *Ccng1* in uninfected MEFs. The αKeap1 ChIP signals at *Cdkn1a* and *Ccng1* were 1.9 and 2.8 higher, on average, in uninfected MEFs that were cultured with BIX01294, than in the same MEFs that were

cultured with vehicle (Figure 2B). The effects of BIX01294 on Keap1 binding to *Cdkn1a* and *Ccng1* in different virus infected MEFs depended on the efficiency of viral inhibition of Keap1 binding at each gene (Figure 2B, Figure 3A). BIX01294 augmented Keap1 binding to *Ifnb1*, *Tnf* and *Il6* mainly in virus infected MEFs, whereas BIX01294 augmented Keap1 binding to *Cdkn1a* and *Ccng1* more efficiently in uninfected MEFs.

BIX01294 effects on virus induced NFκB binding are mediated by Keap1

BIX01294 augments virus induced NFκB binding to cytokine genes in MEFs with intact *Keap1* (14). We examined the mechanisms whereby G9a-GLP inhibitors augment NFκB binding by comparing BIX01294 effects on NFκB p50 and NFκB p65 binding to different genes in MEFs with intact *Keap1* and in *Keap1−/− Nrf2−/−* MEFs. BIX01294 augmented viral induction of NFκB p50 binding to *Ifnb1*, *Tnf* and *Il6* in the 5 different MEFs with intact *Keap1* that were tested (Figure 2B, Figure 3A). The αp50 ChIP signals were 1.6- to 1.9-fold higher, on average, in virus infected MEFs with intact *Keap1* that were cultured with BIX01294 than they were in the same MEFs that were cultured with vehicle. Since BIX01294 had parallel effects on NFκB p50 and Keap1 binding to the cytokine genes, and since Keap1 was essential for NFκB p50 recruitment, it is likely that the effects of BIX01294 on NFκB p50 binding were mediated by BIX01294 effects on Keap1 binding to these genes.

BIX01294 augmented NFκB p65 binding to the genes that were examined in virus infected MEFs with intact *Keap1* (Figure 2B). In contrast, BIX01294 did not augment viral induction of NFκB p65 binding to these genes in *Keap1−/− Nrf2−/−* MEFs. Thus, Keap1 was required for BIX01294 to augment NFκB p65 binding to these genes, whereas Keap1 was not required for viral induction of NFκB p65 binding. These results suggest that G9a-GLP moderates NFκB p65 binding only when they are co-recruited in MEFs with intact *Keap1*. The lack of G9a-GLP inhibitor effects on NFκB p65 binding in *Keap1−/− Nrf2−/−* MEFs, as well as on IRF3 binding in the MEFs that were tested (14), suggest that G9a-GLP inhibitors augmented Keap1 and NFκB subunit binding selectively.

BIX01294 inhibited the increase in H3K9me2 deposition that was induced by virus infection in MEFs with intact *Keap1* (Figure 2B, Figure 3A). In contrast, BIX01294 had no effect on basal H3K9me2 levels in uninfected MEFs or in *Keap1−/− Nrf2−/−* MEFs. BIX01294 had little effect on the αH3 or αH3K27me3 ChIP signals that were examined (Figure 3A, Figure S2). The effects of BIX01294 on Keap1 and NFκB p50 recruitment and on transcription correlated with its effects on H3K9me2 deposition at virus induced genes (*Ifnb1*, *Tnf* and *Il6*), but not at uninduced genes (*Cdkn1a* and *Ccng1*).

Structurally dissimilar G9a-GLP inhibitors augment Keap1 and NFκB p50 binding to virus induced genes.

We compared the effects of different G9a-GLP inhibitors on Keap1 and on NFκB p50 binding to virus induced genes. MS0124 binds to the peptide binding grooves of G9a and GLP, and it is likely to inhibit G9a-GLP methyltransferase activity by competing with its binding to substrate proteins (31). The structurally similar compound MS012 augmented Keap1 and NFκB p50 binding to *Ifnb1*, *Tnf* and *Il6* in the three independent MEFs with

intact *Keap1* that were tested (Figure 3A). The αKeap1 ChIP signals at these genes were 2.3- to 2.7-fold higher, and the αp50 signals were 1.9- to 2.0-fold higher, in virus infected MEFs that were cultured with MS012 than in the same MEFs that were cultured with vehicle. MS012 inhibited H3K9me2 deposition in MEFs with intact *Keap1* (Figure 3A). A lower concentration of MS012 than of BIX01294 was required to augmented Keap1 and NFκB p50 binding and to inhibit H3K9me2 deposition. The parallel effects of BIX01294 and MS012 both on Keap1 and NFκB p50 binding, and on H3K9me2 deposition indicate that these compounds augmented Keap1 and NFκB p50 binding by inhibiting G9a-GLP lysine methyltransferase activities at virus induced genes.

BRD4770 inhibits lysine methyltransferases by competition with S-adenosyl methionine and differs in structure from the other G9a-GLP inhibitors that were tested (32). BRD4770 augmented Keap1 and NFκB p50 binding and inhibited H3K9me2 deposition at virus induced genes in MEFs with intact *Keap1* (Figure 3A). BRD4700 reduced H3K27me3 at these genes both in MEFs with intact Keap1 and in *Keap1−/− Nrf2−/−* MEFs, suggesting that it inhibited other lysine methyltransferases independently of Keap1. UNC0638 as well as UNC0642 augmented Keap1 and NFκB p50 binding at virus induced genes with different efficiencies in different MEFs that correlated with differences in the inhibition of H3K9me2 deposition in those MEFs (Figure 4, Figure S4, Figure S5). Other compounds, including dexamethasone and *tert*-butylhydroquinone (tBHQ) did not augment Keap1 or NFκB p50 binding to virus induced genes, and had no effect on H3K9me2 deposition (Figure 6B, Figure S5). Thus, structurally and mechanistically dissimilar G9a-GLP lysine methyltransferase inhibitors augmented Keap1 and NFκB p50 binding, and inhibited H3K9me2 deposition at virus induced genes.

Compounds that inhibit G9a-GLP through different mechanisms enhance virus induced gene transcription in MEFs with intact *Keap1*

To determine the roles of G9a-GLP methyltransferase activity in virus induced gene transcription, we compared the effects of different G9a-GLP inhibitors on their induction by virus infection. BIX01294, MS0124 and BRD4770 enhanced *Ifnb1*, *Tnf* and *Il6* transcription preferentially in virus infected MEFs with intact *Keap1* (Figure 3B). MS012 enhanced these transcript levels 2.1- to 2.3-fold on average in the two different MEFs with intact *Keap1* that were tested. MS012 reduced or had no significant effect on these transcript levels in two different *Keap1−/− Nrf2−/−* MEFs. BRD4770 enhanced transcription both in MEFs with intact *Keap1* and in *Keap1−/− Nrf2−/−* MEFs (Figure 3B). This could be due to the inhibition of other lysine methyltransferases, including Polycomb repressive complexes 2. BRD4700 reduced H3K27me3 at the genes that were tested both in MEFs with intact *Keap1* and in *Keap1−/− Nrf2−/−* MEFs (Figure 3A). BIX01294, MS012 and BRD4700 had little effect on *Cdkn1a* or *Ccng1* transcription, and they did not increase viral M gene transcript levels. The preferential enhancement of virus induced gene transcription by BIX01294, MS012 and BRD4700 in MEFs with intact *Keap1* suggests that these compounds counteracted the ability of Keap1 to moderate the transcription virus induced genes through the inhibition of G9a-GLP lysine methyltransferase activity.

Keap1 is required for NFκB p50 to bind the Ccl2 enhancer

NFκB p50 binds to many distal enhancers, whereas Keap1 bound to sequences proximal to transcribed regions. We investigated if Keap1 affected NFκB p50 recruitment to the *Ccl2* enhancer. Virus infection induced Keap1 to bind the *Ccl2* promoter and NFκB p50 to bind the *Ccl2* enhancer in MEFs with intact *Keap1*, and not in *Keap1−/− Nrf2−/−* MEFs (Figure 4). Virus infection also induced H3K9me2 deposition at the *Ccl2* promoter and enhancer in MEFs with intact *Keap1*, and not in *Keap1−/− Nrf2−/−* MEFs. G9a-GLP inhibitors augmented Keap1 binding to the *Ccl2* promoter and NFκB p50 binding to the *Ccl2* enhancer in virus infected MEFs with intact *Keap1*, and not in *Keap1−/− Nrf2−/−* MEFs. The augmentation of Keap1 and NFκB p50 binding to the *Ccl2* promoter and enhancer by different G9a-GLP inhibitors correlated with their inhibition of H3K9me2 deposition (Figure 4, Figure S5).

G9a-GLP inhibitors stabilize Keap1 retention in permeabilized MEFs

We evaluated the stability of Keap1 interactions with large complexes in MEFs by measuring the proportion of Keap1 that was retained in MEFs during incubation in buffers that contained different detergents (see diagram above the lanes in Figure 5A). Stronger Keap1 binding to chromatin is predicted to increase its retention in MEFs. MEFs that were cultured with vehicle released almost all Keap1 during incubations with 0.1% and 0.5% Triton X-100 (Figure 5A, Figure S6). In contrast, MEFs that were cultured with BIX01294 retained most of their Keap1 during incubations with 0.1% and 0.5% Triton X-100. Most of the Keap1 as well as histone H3 were released in parallel during incubation with 1% SDS from MEFs that were cultured with BIX01294. A quarter of the Keap1 was retained during incubation with 1% SDS in MEFs that were cultured with BIX01294. Culture with BIX01294 did not affect the retention of cJun, lamin B1 or histone H3 in the MEFs (Figure 5A). The stabilization of Keap1 retention in MEFs that were cultured with BIX01294 suggests that the inhibition of G9a-GLP lysine methyltransferase activity strengthened Keap1 interactions with large complexes in MEFs.

MEFs that were cultured with vehicle released all NFκB p50 during incubations with 0.1% and 0.5% Triton X-100 (Figure 5A, Figure S6). MEFs that were cultured with BIX01294 retained 10% of NFκB p50 during incubations with 0.1% and 0.5% Triton X-100. Culture with BIX01294 did not affect the amount of NFκB p65 that was retained in MEFs. However, culture with BIX01294 altered the electrophoretic mobility of the NFκB p65 that was retained in MEFs (Figure 5A, Figure S6). NFκB p65 that was phosphorylated on S536 was retained more efficiently in MEFs during incubations with detergents than total NFκB p65.

The concentration of BIX01294 and the time of culture that were required to stabilize Keap1 retention in MEFs were similar to those that augmented Keap1 binding to specific genes and inhibited H3K9me2 deposition (Figure 5B, Figure 2B). A lower concentration of MS012 than of BIX01294 was required to stabilize Keap1 retention in MEFs as well as to augment Keap1 binding and inhibit H3K9me2 deposition at specific genes (Figure S6E, Figure 3A). BIX01294 stabilized Keap1 retention both in uninfected and in virus infected MEFs, consistent with the augmentation of Keap1 binding to different genes in uninfected and in virus infected MEFs by BIX01294.

Keap1 and the electrophile tBHQ reduce virus induced gene transcription by altering the recruitment of different NFκB subunits.

Electrophiles can bind Keap1 and affect Keap1 ubiquitin ligase activity. Electrophiles can also reduce the induction of cytokine expression by LPS (33). We investigated if the moderation of virus induced gene transcription by Keap1 was related to the effect of electrophiles on cytokine expression. We compared the effects of Keap1 and of the electrophile tBHQ, which can conjugate covalently to Keap1, on virus induced gene transcription separately and in combination. Virus infection induced higher levels of *Ifnb1* and *Tnf* transcription in *Keap1*$^{-/-}$ *Nrf2*$^{-/-}$ MEFs than in MEFs with intact *Keap1*, whether these MEFs were cultured with vehicle or with tBHQ (Figure 6A). tBHQ reduced and delayed the peak *Ifnb1* and *Tnf* transcript levels to a similar extent both in MEFs with intact *Keap1* and in *Keap1*$^{-/-}$ *Nrf2*$^{-/-}$ MEFs. tBHQ abolished viral induction of *Il6* transcription in these MEFs.

tBHQ did not alter Keap1 recruitment to cytokine genes upon virus infection (Figure 6B). BIX01294 augmented Keap1 binding to these genes also in MEFs that were cultured with tBHQ. It is likely that BIX01294 augmented Keap1 binding to these genes by mechanisms that were unrelated to electrophile responses. The independent effects of Keap1 and of tBHQ on *Ifnb1* and *Tnf* transcription, and the lack of tBHQ effects on Keap1 recruitment to virus induced genes suggest that Keap1 and tBHQ reduced the transcription of these genes through independent mechanisms.

We compared the effects of Keap1 and of tBHQ on NFκB subunit recruitment to virus induced genes. Keap1 was required for NFκB p50 recruitment to virus induced genes, whereas tBHQ had no effect on NFκB p50 recruitment to these genes (Figure 6B). In contrast, tBHQ inhibited NFκB p65 recruitment to these genes both in MEFs with intact *Keap1* and in *Keap1*$^{-/-}$ *Nrf2*$^{-/-}$ MEFs, whereas Keap1 did not affect NFκB p65 recruitment to these genes in the absence of BIX01294. Moreover, tBHQ blocked the augmentation of NFκB p65 binding by BIX01294, whereas it had no effect on the augmentation of NFκB p50 binding by BIX01294 in the same MEFs. Whereas both Keap1 and tBHQ reduced the transcription of virus induced genes and altered NFκB subunit recruitment to these genes, the molecular mechanisms for these effects were distinct.

Discussion

These experiments have uncovered a regulatory circuit that moderates the transcription of virus induced genes. Virus infection actuated this circuit by inducing Keap1 to bind to virus induced genes. The parallel actuation of mechanisms that activate and those that moderate the transcription of virus induced genes can shape the timing and the amplitude of virus induced gene transcription in response to signals that modulate their expression.

Sendai virus infection induced Keap1 to bind to genes whose transcription was induced by virus infection selectively. Keap1 moderated the transcription of these genes, and Keap1 was required for G9a-GLP and NFκB p50 recruitment and H3K9me2 deposition at the genes, upon virus infection. G9a-GLP inhibitors enhanced virus induced gene transcription in MEFs with intact *Keap1* selectively, and augmented Keap1 and NFκB p50 binding at

these genes. The coordinate recruitment of Keap1, G9a-GLP and NFκB p50 to virus induced genes, and the reversal of Keap1 moderation of virus induced transcription by G9a-GLP inhibitors, suggest that these proteins function in concert to moderate the transcription of virus induced genes.

The induction of G9a-GLP recruitment and H3K9me2 deposition at virus induced genes were unexpected because these chromatin states are conventionally associated with gene silencing. Countermanding this convention, trivalent influenza virus vaccination also increases H3K9me2 levels in CD34+ progenitors and monocyte subsets of clinical trial participants (34). This increase in H3K9me2 correlates with reduced chromatin accessibility and lower cytokine induction in PBMCs from vaccinated subjects. H3K9me2 deposition could be a common response to virus infection that moderates the transcription of virus induced genes.

Since Keap1 does not contain a recognized DNA binding domain, it is likely that the contrasting effects of virus infection on Keap1 binding to virus induced versus uninduced genes were mediated by interactions with different DNA binding proteins at different genes. The higher levels and increased stability of Keap1 binding to chromatin in MEFs that were cultured with G9a-GLP inhibitors suggests that lysine methylation by G9a-GLP alters some of these interactions. The molecular mechanisms that induced Keap1 to bind at virus induced genes, and those that reduced Keap1 binding at cell cycle associated genes upon virus infection remain unknown.

Viral induction of Keap1 binding to *Ifnb1*, *Tnf* and *Il6*, and the higher levels of these transcripts in *Keap1*−/− *Nrf2*−/− MEFs than in MEFs with intact *Keap1* suggest that Keap1 moderated *Ifnb1*, *Tnf* and *Il6* transcription in virus infected MEFs by binding to these genes. The absence of G9a-GLP and NFκB p50 recruitment, and the higher levels of virus induced gene transcription in *Keap1*−/− *Nrf2*−/− MEFs suggest that Keap1 moderated the transcription of virus induced genes by facilitating G9a-GLP and NFκB p50 recruitment to these genes. Keap1 forms complexes with NFκB p50 and NFκB p65 that can bind chromatin in living cells, demonstrating that they can be recruited in concert (14). G9a and GLP co-precipitate with NFκB subunits from cell extracts, suggesting that they could also be recruited in concert (18, 35). Virus infection had opposite effects on Keap1 versus NFκB subunit binding at cell cycle associated genes, and G9a-GLP bound to flanking regions where no Keap1 or NFκB binding was detected, indicating that these proteins can bind chromatin separately.

G9a-GLP inhibitors augmented Keap1 and NFκB recruitment, enhanced virus induced gene transcription, and inhibited H3K9me2 deposition in parallel at virus induced genes. G9a-GLP inhibitors enhanced virus induced gene transcription and inhibited H3K9me2 deposition only in MEFs with intact *Keap1*. The correspondence between G9a-GLP recruitment by Keap1 and the enhancement of virus induced transcription by G9a-GLP inhibitors suggests that the moderation of virus induced gene transcription by Keap1 required G9a-GLP recruitment to these genes.

G9a-GLP inhibitors augmented both Keap1 and NFκB recruitment to virus induced genes and enhanced the transcription of these genes upon virus infection, through mechanisms that correlated with their inhibition of H3K9me2 deposition. In contrast, G9a-GLP inhibitors augmented Keap1 recruitment to cell cycle genes through mechanisms that did not correlate with changes in H3K9me2 deposition. These results suggest that G9a-GLP moderated Keap1 and NFκB recruitment and virus induced transcription both through H3K9 dimethylation as well as through other G9a-GLP lysine methyltransferase substrates.

G9a-GLP inhibitors augmented Keap1 binding to specific genes and stabilized Keap1 retention in permeabilized MEFs. Both effects required similar times of G9a-GLP inhibition and the relative potencies of different G9a-GLP inhibitors were similar for each of these effects. Keap1 retention in HeLa cells varies at different times after release from cell cycle arrest, which has been interpreted to reflect changes in Keap1 binding to chromatin at different stages of the cell cycle (36). Docosahexaenoic acid stabilizes Keap1 retention in human primary monocyte-derived macrophages and reduces *CXCL10* and *CXCL11* induction by LPS (37). The effects of several G9a-GLP inhibitors on Keap1 binding to specific genes and on Keap1 retention in permeabilized MEFs suggest that G9a-GLP lysine methyltransferase activity moderates both of these characteristics of Keap1.

Keap1, G9a-GLP, and NFκB p50 bind to virus induced genes at higher levels in *Nrf2−/−* MEFs compared to MEFs with intact Nrf2 (14). The effects of *Nrf2−/−* deletions on Keap1 recruitment suggest that Nrf2 counteracts viral induction of Keap1 binding. Both the loss of Keap1 binding upon *Keap1−/−* deletions as well as the gain in Keap1 binding upon *Nrf2−/−* deletions are reflected by parallel changes in G9a-GLP and NFκB p50 recruitment (14). The interdependence of Keap1, G9a-GLP and NFκB p50 binding to, and regulation of, virus induced genes suggest that these proteins are part of a regulatory network whose integrated function moderates the transcription of virus induced genes.

The effects of Keap1 mutations in human cancers and in mice have been attributed to changes in Nrf2 activity (1–7, 38). The observations that Keap1 can regulate immunomodulatory gene transcription directly as well as indirectly suggest that the physiological functions of Keap1 are mediated by multiple mechanisms. Compounds that alter Keap1 moderation of virus induced gene transcription could be useful for the prophylaxis and the treatment of infectious diseases and immune disorders.

Supplementary Material

Refer to Web version on PubMed Central for supplementary material.

Acknowledgments.

The authors thank Masayuki Yamamoto and Thomas Kensler for mouse strains with the *Keap1-* and the *Nrf2-* deletion alleles. The authors thank Huai Deng for preparing some of the MEFs and for investigating the effects of tBHQ on Keap1 and Nrf2 binding to electrophile response genes.

References

1. Wakabayashi N, Itoh K, Wakabayashi J, Motohashi H, Noda S, Takahashi S, et al. Keap1-null mutation leads to postnatal lethality due to constitutive Nrf2 activation. Nat Genet. 2003;35(3):238–45. [PubMed: 14517554]
2. Suzuki T, Seki S, Hiramoto K, Naganuma E, Kobayashi EH, Yamaoka A, et al. Hyperactivation of Nrf2 in early tubular development induces nephrogenic diabetes insipidus. Nature Communications. 2017;8:14577.
3. Klemm P, Rajendiran A, Fragoulis A, Wruck C, Schippers A, Wagner N, et al. Nrf2 expression driven by Foxp3 specific deletion of Keap1 results in loss of immune tolerance in mice. Eur J Immunol. 2020;50(4):515–24. [PubMed: 31840803]
4. Blake DJ, Singh A, Kombairaju P, Malhotra D, Mariani TJ, Tuder RM, et al. Deletion of Keap1 in the lung attenuates acute cigarette smoke-induced oxidative stress and inflammation. American Journal of Respiratory Cell and Molecular Biology. 2010;42(5):524–36. [PubMed: 19520915]
5. Kong X, Thimmulappa R, Craciun F, Harvey C, Singh A, Kombairaju P, et al. Enhancing Nrf2 Pathway by Disruption of Keap1 in Myeloid Leukocytes Protects against Sepsis. American Journal of Respiratory and Critical Care Medicine. 2011;184(8):928–38. [PubMed: 21799073]
6. Noel S, Martina MN, Bandapalle S, Racusen LC, Potteti HR, Hamad ARA, et al. T Lymphocyte–Specific Activation of Nrf2 Protects from AKI. Journal of the American Society of Nephrology. 2015;26:2989–3000. [PubMed: 26293820]
7. Nezu M, Souma T, Yu L, Suzuki T, Saigusa D, Ito S, et al. Transcription factor Nrf2 hyperactivation in early-phase renal ischemia-reperfusion injury prevents tubular damage progression. Kidney International. 2017;91(2):387–401. [PubMed: 27789056]
8. Awuh JA, Haug M, Mildenberger J, Marstad A, Do CP, Louet C, et al. Keap1 regulates inflammatory signaling in Mycobacterium avium-infected human macrophages. Proc Natl Acad Sci U S A. 2015;112(31):E4272–80. [PubMed: 26195781]
9. Lv P, Xue P, Dong J, Peng H, Clewell R, Wang A, et al. Keap1 silencing boosts lipopolysaccharide-induced transcription of interleukin 6 via activation of nuclear factor kappaB in macrophages. Toxicol Appl Pharmacol. 2013;272(3):697–702. [PubMed: 23906629]
10. Kobayashi EH, Suzuki T, Funayama R, Nagashima T, Hayashi M, Sekine H, et al. Nrf2 suppresses macrophage inflammatory response by blocking proinflammatory cytokine transcription. Nat Commun. 2016;7:11624. [PubMed: 27211851]
11. Davidson S, Coles M, Thomas T, Kollias G, Ludewig B, Turley S, et al. Fibroblasts as immune regulators in infection, inflammation and cancer. Nature Reviews Immunology. 2021;21(11):704–17.
12. Krausgruber T, Fortelny N, Fife-Gernedl V, Senekowitsch M, Schuster LC, Lercher A, et al. Structural cells are key regulators of organ-specific immune responses. Nature. 2020;583(7815):296–302. [PubMed: 32612232]
13. Boyd DF, Allen EK, Randolph AG, Guo X-zJ, Weng Y, Sanders CJ, et al. Exuberant fibroblast activity compromises lung function via ADAMTS4. Nature. 2020;587(7834):466–71. [PubMed: 33116313]
14. Burns VE, Kerppola TK. Virus Infection Induces Keap1 Binding to Cytokine Genes, Which Recruits NF-κB p50 and G9a-GLP and Represses Cytokine Transcription. The Journal of Immunology. 2021;207(5):1437–47. [PubMed: 34400522]
15. Tachibana M, Sugimoto K, Nozaki M, Ueda J, Ohta T, Ohki M, et al. G9a histone methyltransferase plays a dominant role in euchromatic histone H3 lysine 9 methylation and is essential for early embryogenesis. Genes Dev. 2002;16(14):1779–91. [PubMed: 12130538]
16. Tachibana M, Ueda J, Fukuda M, Takeda N, Ohta T, Iwanari H, et al. Histone methyltransferases G9a and GLP form heteromeric complexes and are both crucial for methylation of euchromatin at H3-K9. Genes Dev. 2005;19(7):815–26. [PubMed: 15774718]
17. Gazzar ME, Yoza BK, Chen X, Hu J, Hawkins GA, McCall CE. G9a and HP1 Couple Histone and DNA Methylation to TNFα Transcription Silencing during Endotoxin Tolerance. Journal of Biological Chemistry. 2008;283(47):32198–208. [PubMed: 18809684]

18. Ea C-K, Hao S, Yeo KS, Baltimore D. EHMT1 Protein Binds to Nuclear Factor-κB p50 and Represses Gene Expression. Journal of Biological Chemistry. 2012;287(37):31207–17. [PubMed: 22801426]
19. Fang TC, Schaefer U, Mecklenbrauker I, Stienen A, Dewell S, Chen MS, et al. Histone H3 lysine 9 di-methylation as an epigenetic signature of the interferon response. The Journal of Experimental Medicine. 2012;209:661–9. [PubMed: 22412156]
20. Lehnertz B, Northrop JP, Antignano F, Burrows K, Hadidi S, Mullaly SC, et al. Activating and inhibitory functions for the histone lysine methyltransferase G9a in T helper cell differentiation and function. J Exp Med. 2010;207(5):915–22. [PubMed: 20421388]
21. Antignano F, Braam M, Hughes MR, Chenery AL, Burrows K, Gold MJ, et al. G9a regulates group 2 innate lymphoid cell development by repressing the group 3 innate lymphoid cell program. Journal of Experimental Medicine. 2016;213(7):1153–62. [PubMed: 27298444]
22. Mourits VP, van Puffelen JH, Novakovic B, Bruno M, Ferreira AV, Arts RJW, et al. Lysine methyltransferase G9a is an important modulator of trained immunity. Clinical & Translational Immunology. 2021;10(2):e1253. [PubMed: 33708384]
23. Dissanayake D, Hall H, Berg-Brown N, Elford AR, Hamilton SR, Murakami K, et al. Nuclear factor-kappaB1 controls the functional maturation of dendritic cells and prevents the activation of autoreactive T cells. Nat Med. 2011;17(12):1663–7. [PubMed: 22081022]
24. Fliegauf M L.Bryant V, Frede N, Slade C, Woon S-T, Lehnert K, et al. Haploinsufficiency of the NF-κB1 Subunit p50 in Common Variable Immunodeficiency. The American Journal of Human Genetics. 2015;97(3):389–403. [PubMed: 26279205]
25. Schipp C, Nabhani S, Bienemann K, Simanovsky N, Kfir-Erenfeld S, Assayag-Asherie N, et al. Specific antibody deficiency and autoinflammatory disease extend the clinical and immunological spectrum of heterozygous NFKB1 loss-of-function mutations in humans. Haematologica. 2016;101(10):e392–e6. [PubMed: 27365489]
26. Deng H, Kerppola TK. Regulation of Drosophila metamorphosis by xenobiotic response regulators. PLoS Genetics. 2013;9(2):e1003263. [PubMed: 23408904]
27. Deng H, Kerppola TK. Visualization of the Drosophila dKeap1-CncC interaction on chromatin illumines cooperative, xenobiotic-specific gene activation. Development. 2014;141(16):3277–88. [PubMed: 25063457]
28. Itoh K, Chiba T, Takahashi S, Ishii T, Igarashi K, Katoh Y, et al. An Nrf2/small Maf heterodimer mediates the induction of phase II detoxifying enzyme genes through antioxidant response elements. Biochem Biophys Res Commun. 1997;236(2):313–22. [PubMed: 9240432]
29. Kubicek S, O'Sullivan RJ, August EM, Hickey ER, Zhang Q, Teodoro ML, et al. Reversal of H3K9me2 by a small-molecule inhibitor for the G9a histone methyltransferase. Mol Cell. 2007;25(3):473–81. [PubMed: 17289593]
30. Chang Y, Zhang X, Horton JR, Upadhyay AK, Spannhoff A, Liu J, et al. Structural basis for G9a-like protein lysine methyltransferase inhibition by BIX-01294. Nature Structural & Molecular Biology. 2009;16(3):312–7.
31. Xiong Y, Li F, Babault N, Dong A, Zeng H, Wu H, et al. Discovery of Potent and Selective Inhibitors for G9a-Like Protein (GLP) Lysine Methyltransferase. J Med Chem. 2017;60(5):1876–91. [PubMed: 28135087]
32. Yuan Y, Wang Q, Paulk J, Kubicek S, Kemp MM, Adams DJ, et al. A Small-Molecule Probe of the Histone Methyltransferase G9a Induces Cellular Senescence in Pancreatic Adenocarcinoma. ACS Chemical Biology. 2012;7(7):1152–7. [PubMed: 22536950]
33. Mills EL, Ryan DG, Prag HA, Dikovskaya D, Menon D, Zaslona Z, et al. Itaconate is an anti-inflammatory metabolite that activates Nrf2 via alkylation of KEAP1. Nature. 2018;556(7699):113–7. [PubMed: 29590092]
34. Wimmers F, Donato M, Kuo A, Ashuach T, Gupta S, Li C, et al. The single-cell epigenomic and transcriptional landscape of immunity to influenza vaccination. Cell. 2021;184(15):3915–35.e21. [PubMed: 34174187]
35. Chen X, El Gazzar M, Yoza BK, McCall CE. The NF-kappaB factor RelB and histone H3 lysine methyltransferase G9a directly interact to generate epigenetic silencing in endotoxin tolerance. The Journal of biological chemistry. 2009;284(41):27857–65. [PubMed: 19690169]

36. Mulvaney KM, Matson JP, Siesser PF, Tamir TY, Goldfarb D, Jacobs TM, et al. Identification and Characterization of MCM3 as a Kelch-like ECH-associated Protein 1 (KEAP1) Substrate. Journal of Biological Chemistry. 2016;291(45):23719–33. [PubMed: 27621311]

37. Mildenberger J, Johansson I, Sergin I, Kjobli E, Damas JK, Razani B, et al. N-3 PUFAs induce inflammatory tolerance by formation of KEAP1-containing SQSTM1/p62-bodies and activation of NFE2L2. Autophagy. 2017;13(10):1664–78. [PubMed: 28820283]

38. Singh A, Misra V, Thimmulappa RK, Lee H, Ames S, Hoque MO, et al. Dysfunctional KEAP1-NRF2 interaction in non-small-cell lung cancer. PLoS Med. 2006;3(10):e420. [PubMed: 17020408]

- Representative data are presented in the figures and supplemental files. All original data that contributed to the analysis are retained and are available from the corresponding author on reasonable request. The reagents used are available from commercial suppliers.
- The work was funded in part by National Institutes of Health National Institute on Drug Abuse (DA030339).
- The authors declare that competing interests did not influence the design or the interpretation of the experiments.
- All experiments with live mice were approved by the Institutional Animal Care & Use Committee at University of Michigan

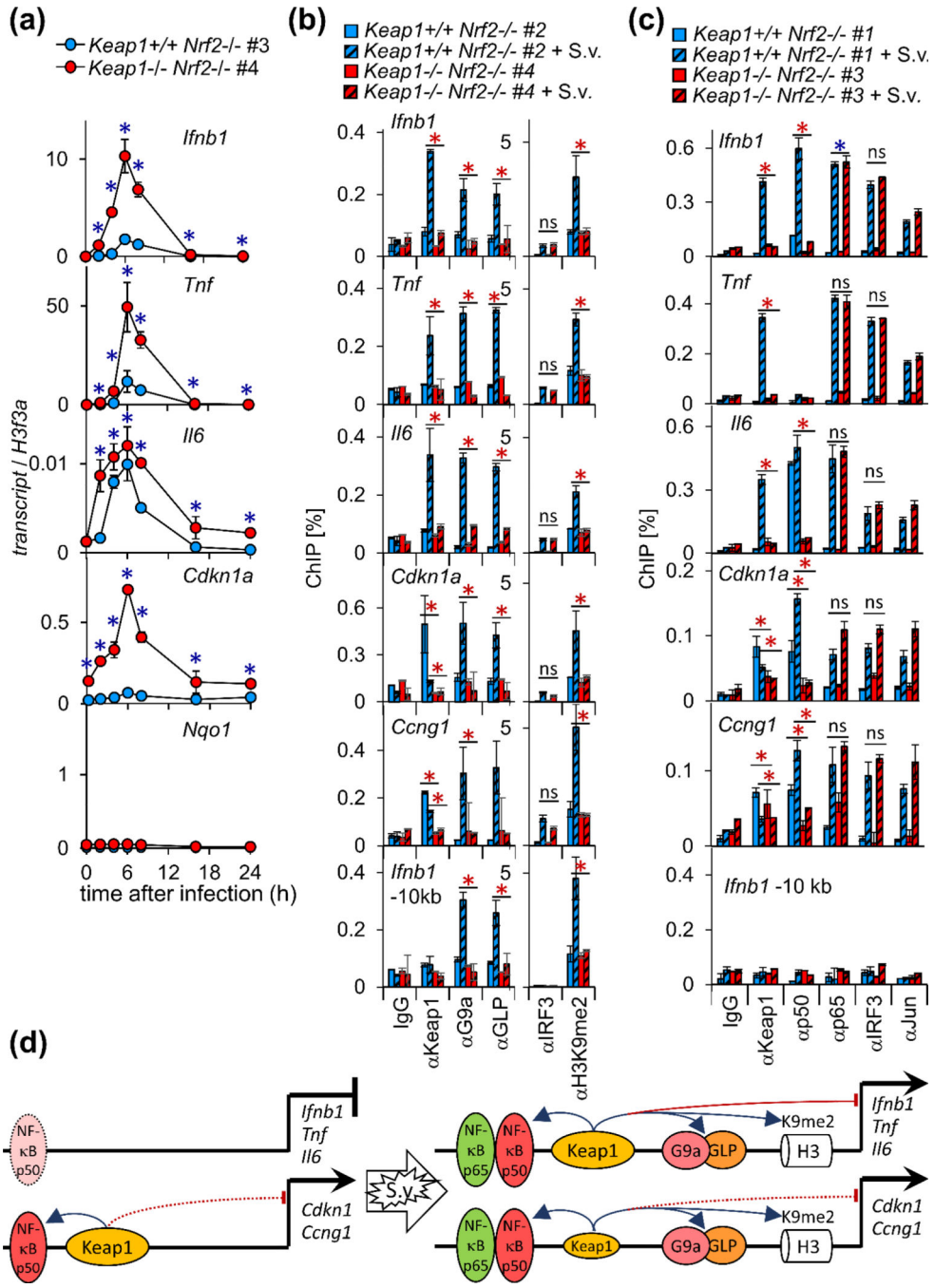

Figure 1. Virus infection induces higher cytokine transcript levels in MEFs with *Keap1*−/− deletions than in MEFs with intact *Keap1*, and has opposite effects on Keap1 recruitment to cytokine *versus* cell cycle genes; Keap1 is required for G9a, GLP and NFκB p50 recruitment and for H3K9me2 deposition.

(a) Virus infection induces higher levels of cytokine transcripts in *Keap1*−/− *Nrf2*−/− MEFs than in MEFs with intact *Keap1*. MEFs with intact *Keap1* (blue) and MEFs with *Keap1*−/− deletions (red), each with *Nrf2*−/− deletions, were infected with Sendai virus. The levels of the transcripts indicated in the graphs were measured by RT-qPCR at the times after virus infection indicated on the bottom graph. The line graphs show the results (mean±2*SD) of a

representative experiment in which *Keap1+/+ Nrf2−/−* #3 and *Keap1−/− Nrf2−/−* #4 MEFs were compared. The # after each genotype refers to a MEF population that was isolated from a specific embryo. The reproducibility of Keap1 effects on the RT-qPCR transcript signals were evaluated in 3–7 different sets of MEFs by performing two-factor ANOVA analyses (* $p<0.0005$). The effects of Keap1 on virus induced and on electrophile response gene transcription in the presence and in the absence of Nrf2 are compared in Figure S1.

(b) Virus infection has opposite effects on Keap1 binding to cytokine versus cell cycle genes, and Keap1 is required for G9a and GLP recruitment and for H3K9me2 deposition upon virus infection. MEFs with intact *Keap1* (blue bars) and MEFs with *Keap1−/−* deletions (red bars), each with *Nrf2−/−* deletions, were infected with mock (solid bars) or Sendai virus (S.v., striped bars). The levels of Keap1, G9a, GLP and IRF3 binding, and of H3K9me2 were measured 6 hours after infection at the genes indicated in the graphs using the antibodies indicated. The bar graphs show the results (mean±2*SD) of a representative experiment in which *Keap1+/+ Nrf2−/−* #2 and *Keap1−/− Nrf2−/−* #4 MEFs were compared. The reproducibility of *Keap1−/−* effects on G9a, GLP, IRF3, and H3K9me2 ChIP signals were evaluated in 2–5 different sets of MEFs by two-factor ANOVA analyses (* $p<0.001$, blue – increase, red – decrease).

(c) Keap1 is required for NFκB p50 recruitment both in virus infected and in uninfected MEFs. MEFs with intact *Keap1* (blue bars) and MEFs with *Keap1−/−* deletions (red bars), each with *Nrf2−/−* deletions, were infected with mock (solid bars) or Sendai virus (S.v. striped bars). The levels of NFκB p50, NFκB p65, IRF3 and cJun binding were measured 6 hours after infection at the genes indicated in the graphs using the antibodies indicated at the bottom. The bar graphs show the results (mean±2*SD) of a representative experiment in which *Keap1+/+ Nrf2−/−* #1 and *Keap1−/− Nrf2−/−* #3 MEFs were compared. The reproducibility of *Keap1−/−* effects on NFκB p50 and NFκB p65 ChIP binding signals were evaluated in 4–6 different sets of MEFs by two-factor ANOVA analyses (* $p<0.001$, blue – increase, red – decrease).

(d) The diagrams compare effects of virus infection on Keap1 recruitment, and Keap1 effects on G9a, GLP, NFκB p50 and H3K9me2 levels, and on transcription at cytokine *versus* cell cycle associated genes. The blue arrows indicate effects that are required for binding or for deposition. The red arcs and bars indicate effects that moderate transcription. Dotted lines and ovals indicate effects and binding that were different at different genes.

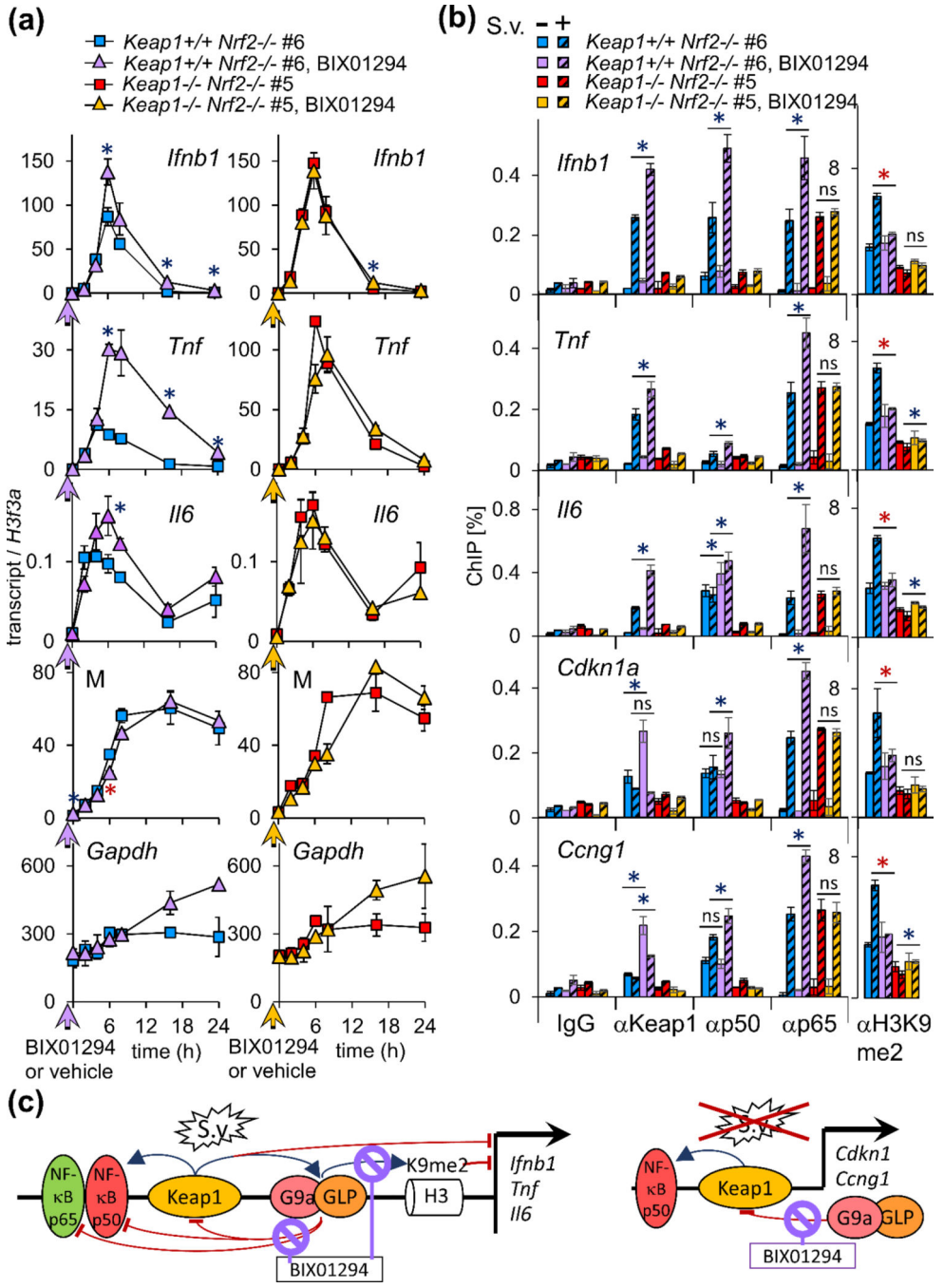

Figure 2. Inhibition of G9a-GLP enhances the transcription of virus induced genes in MEFs with intact *Keap1*, and augments Keap1 binding to different genes in uninfected versus virus infected MEFs.

(a) BIX01294 enhances the transcription of virus induced genes in MEFs with intact *Keap1* selectively. MEFs with intact *Keap1* (left graphs) and MEFs with *Keap1−/−* deletions (right graphs), each with *Nrf2−/−* deletions, were cultured with 20 μM BIX01294 or vehicle starting an hour before virus infection (arrowhead on time axis). The levels of the transcripts indicated in the graphs were measured at the times after virus infection indicated at the bottom. The line graphs show the results of a representative experiment in which

Keap1+/+ Nrf2−/− #6 and *Keap1−/− Nrf2−/−* #5 MEFs were compared. The reproducibility of BIX01294 effects on RT-qPCR transcript signals were evaluated in 2–4 different sets of MEFs by two-factor ANOVA analyses (* $p<0.001$, blue – increase, red – decrease).

(b) BIX01294 augments Keap1 binding to different genes in virus infected and in uninfected MEFs. MEFs with intact *Keap1* and MEFs with *Keap1−/−* deletions, each with *Nrf2−/−* deletions, were cultured with 20 μM BIX01294 or vehicle for an hour before mock (solid bars) or virus (striped bars) infection. The levels of Keap1, NFκB p50, NFκB p65, and H3K9me2 were measured 6 hours after infection at the genes indicated in the graphs using the antibodies indicated. The bar graphs show the results of a representative experiment in which *Keap1+/+ Nrf2−/−* #6 and *Keap1−/− Nrf2−/−* #5 MEFs were compared. The reproducibility of BIX01294 effects on Keap1, NFκB p50 and NFκB p65, and H3K9me2 ChIP signals were evaluated in 2–5 different sets of MEFs by two-factor ANOVA analyses (* $p<0.005$, blue – increase, red – decrease). Keap1 binding to chromatin and BIX01294 effects on Keap1 binding were measured using several different anti-Keap1 antibodies as shown in Figure S2.

(c) The diagrams compare BIX01294 effects on Keap1, NFκB p50, and H3K9me2 levels, and on transcription at cytokine genes in virus infected MEFs and at cell cycle associated genes in uninfected MEFs. The blue arrows indicate effects that are required for binding or for deposition. The red arcs and bars indicate effects that inhibit or moderate recruitment, deposition, or transcription.

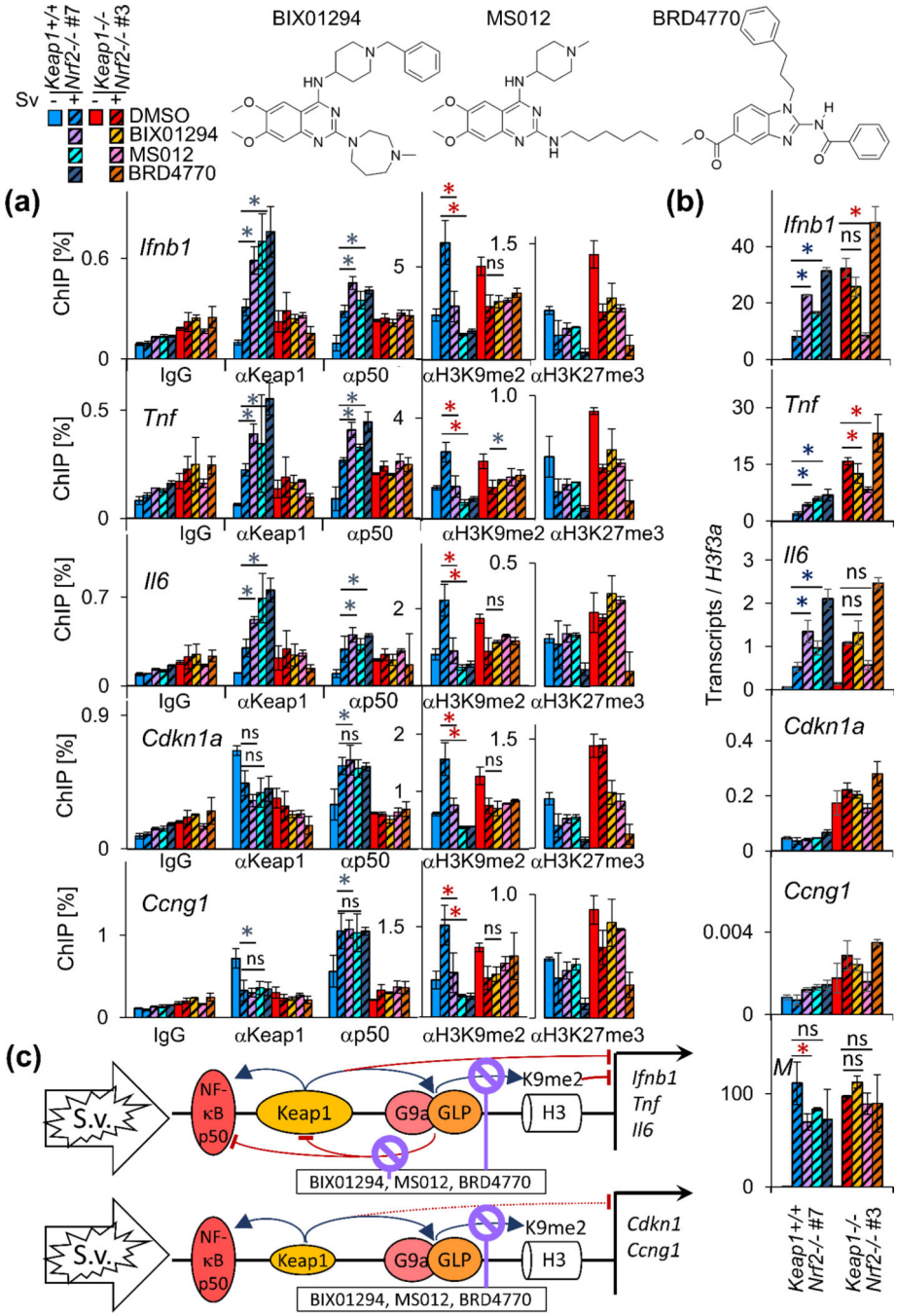

Figure 3. Structurally dissimilar G9a-GLP inhibitors augment Keap1 and NFκB p50 binding to virus induced genes, and enhance the transcription of virus induced genes in MEFs with intact *Keap1*.

(a) Different G9a-GLP inhibitors have parallel effects on Keap1 and NFκB p50 binding to virus induced genes in MEFs with intact *Keap1*. MEFs with intact *Keap1* (cool colors) and MEFs with *Keap1−/−* deletions (warm colors), each with *Nrf2−/−* deletions, were cultured with 20 μM BIX01294 starting an hour before infection, or with 1 μM MS012, 20 μM BRD4770 or vehicle starting 48 hours before infection. The Keap1, NFκB p50, H3K9me2 and H3K27me3 levels were measured 6 hours after mock (solid bars) or virus (striped bars)

infection at the genes that are indicated in the graphs using the antibodies indicated at the bottom. The bar graphs show the results of a representative experiment in which *Keap1+/+ Nrf2−/−* #7 and *Keap1−/− Nrf2−/−* #3 MEFs were compared. The MEFs that were analyzed in panels A and B were cultured in parallel, and the legend at the top of the figure applies to both panels. The reproducibility of BIX01294 and MS012 effects on Keap1, NFκB p50, and H3K9me2 ChIP signals were evaluated in 2–4 different sets of MEFs by two-factor ANOVA analyses (* $p<0.005$, blue – increase, red – decrease).

(b) Several G9a-GLP inhibitors have distinct effects on virus induced gene transcription in MEFs with intact *Keap1 versus* MEFs with *Keap1−/−* deletions. MEFs with intact *Keap1* (cool colors) and MEFs with *Keap1−/−* deletions (warm colors), each with *Nrf2−/−* deletions, were cultured with 20 μM BIX01294 starting an hour before infection, or with 1 μM MS012, 20 μM BRD4770 or vehicle starting 48 hours before infection. The levels of the transcripts indicated in the graphs were measured 6 hours after mock (solid bars) or virus (striped bars) infection. The graphs show the results of a representative experiment in which *Keap1+/+ Nrf2−/−* #7 and *Keap1−/− Nrf2−/−* #3 MEFs were compared. The reproducibility of BIX01294 and MS012 effects on RT-qPCR transcript signals were evaluated in 2–4 different sets of MEFs by two-factor ANOVA analyses (* $p<0.001$, blue – increase, red – decrease). UNC0638 and UNC0642 effects on Keap1, NFκB p50, and H3K9me2 levels, and on virus induced gene transcription are analyzed in Figure S4.

(c) The diagrams compare effects of G9a-GLP inhibitors on Keap1, NFκB p50, and H3K9me2 levels, and on transcription at cytokine *versus* cell cycle associated genes in virus infected MEFs. The blue arrows indicate effects that are required for binding or for deposition. The red arcs and bars indicate effects that inhibit or moderate recruitment, deposition, or transcription.

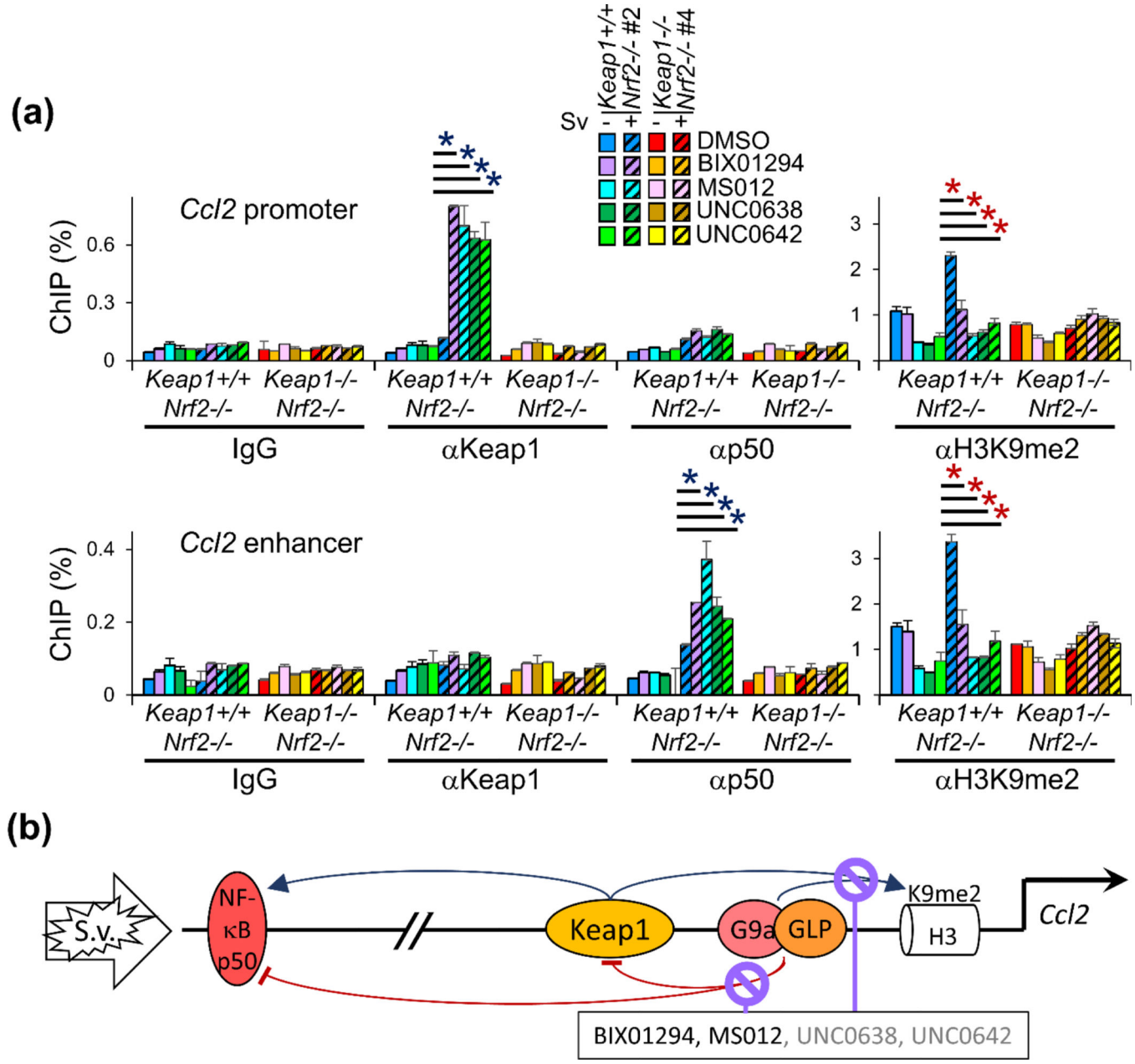

Figure 4. G9a-GLP inhibitors augment Keap1 binding to the *Ccl2* promoter and NFκB p50 binding to the *Ccl2* enhancer in virus infected MEFs.

(a) Keap1 binds to the Ccl2 promoter and is required for NFkB p50 to bind the Ccl2 enhancer and for H3K9me2 deposition. MEFs with intact Keap1 (cool colors) and MEFs with *Keap1−/−* deletions (warm colors), each with *Nrf2−/−* deletions, were cultured for one hour with 20 μM BIX01294, or for 48 hours with 1 μM MS012, 10 μM UNC0638, 10 μM UNC0642, or vehicle before infection. The Keap1, NFkB p50, and H3K9me2 levels were measured 6 h after mock (solid bars) or virus (striped bars) infection at the *Ccl2* promoter (upper graph) and at the *Ccl2* enhancer (lower graph) using the antibodies indicated. The graphs show the results of a representative experiment in which *Keap1+/+ Nrf2−/−* #2 and *Keap1−/− Nrf2−/−* #4 MEFs were compared. The reproducibility of G9a-GLP inhibitor

effects on Keap1, NFkB p50, and H3K9me2 ChIP signals were evaluated in 2 experiments by two-factor ANOVA analyses (* $p<0.005$, blue – increase, red – decrease). The effects of these G9a-GLP inhibitors on Keap1, NFkB p50, and H3K9me2 levels at additional genes are compared in Figure S5.

(b) The diagram depicts effects of virus infection and G9a-GLP inhibitors on Keap1, NFκB p50, and H3K9me2 levels at the *Ccl2* enhancer and promoter in virus infected MEFs. The blue arrows indicate effects that are required for binding or for deposition. The red arcs and bars indicate effects that inhibit or moderate binding or deposition. Compounds that had different effects in different experiments are indicated in grey type.

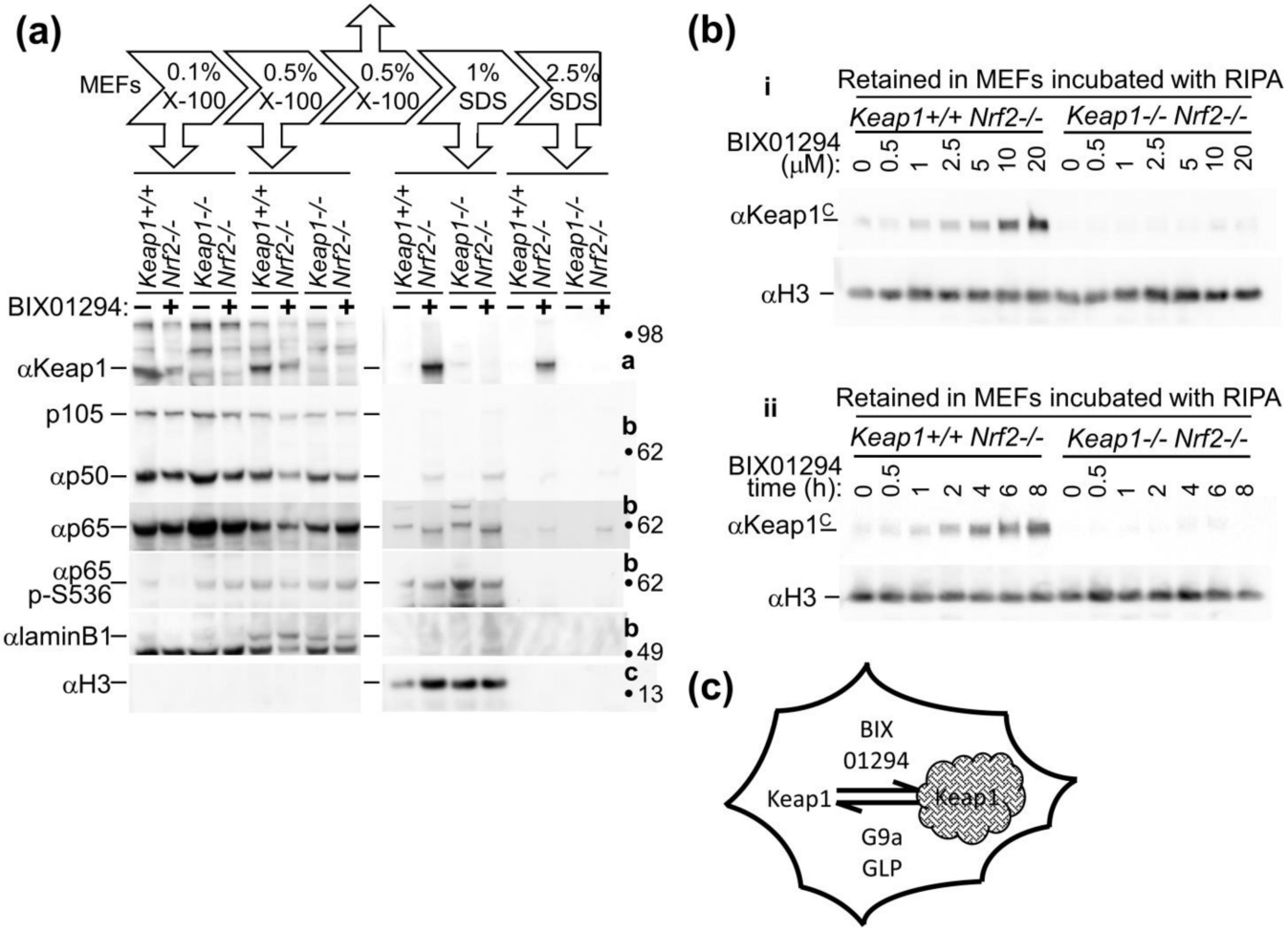

Figure 5. G9a-GLP inhibition stabilizes Keap1 retention in permeabilized MEFs.

(a) Culture with BIX01294 stabilizes Keap1 and NFκB p50 retention in MEFs that are incubated with detergents. The MEFs that are indicated above the lanes were cultured with vehicle (–) or with 20 μM BIX01294 (+) for 48 hours. After culture, the MEFs were incubated sequentially in buffers that contained the detergents indicated above the lanes (see Materials and Methods in supplementary information). The proteins that were released into the supernatant during incubation with each detergent were analyzed by immunoblotting using the antibodies indicated to the left of the images. The cell pellets that contained the proteins that were retained in the MEFs were incubated in the subsequent buffer with more or stronger detergent. No proteins were detected in the lanes that were loaded with supernatants from a second incubation with 0.5% Triton X-100 (up arrow in the diagram at the top), and those lanes are not shown. The same samples were analyzed on several membranes as indicated to the right of the images (a, b, c). The images show results from a representative experiment in which *Keap1+/+ Nrf2−/−* #2 and *Keap1−/− Nrf2−/−* #4 MEFs were compared. The mobilities of molecular weight markers are indicated to the right of the images.

(b) Effects of the concentration of BIX01294 and of the time of culture with BIX01294 on Keap1 retention in MEFs. The MEFs that are indicated above the images were cultured

with the indicated concentrations (μM) of BIX01294 for 4 h (i, upper panel), and for the indicated times (h) with 20 μM BIX01294 (ii, lower panel). After culture, the MEFs were incubated in RIPA buffer, and the proteins that were retained in the MEFs were analyzed by immunoblotting. The images show αKeap1^{C} and αH3 immunoblots of the proteins that were retained in the MEFs. The images show the results from a representative experiment in which *Keap1+/+* Nrf2−/− #8 and *Keap1−/−* Nrf2−/− #5 MEFs were compared. The proteins that were released from these MEFs are shown in Figure S6D and the effects of BIX01294 on protein retention are quantified and compared in different MEFs and with different detergents in Figure S6.

(c) The diagram illustrates the stabilization of Keap1 retention in MEFs by G9a-GLP inhibition.

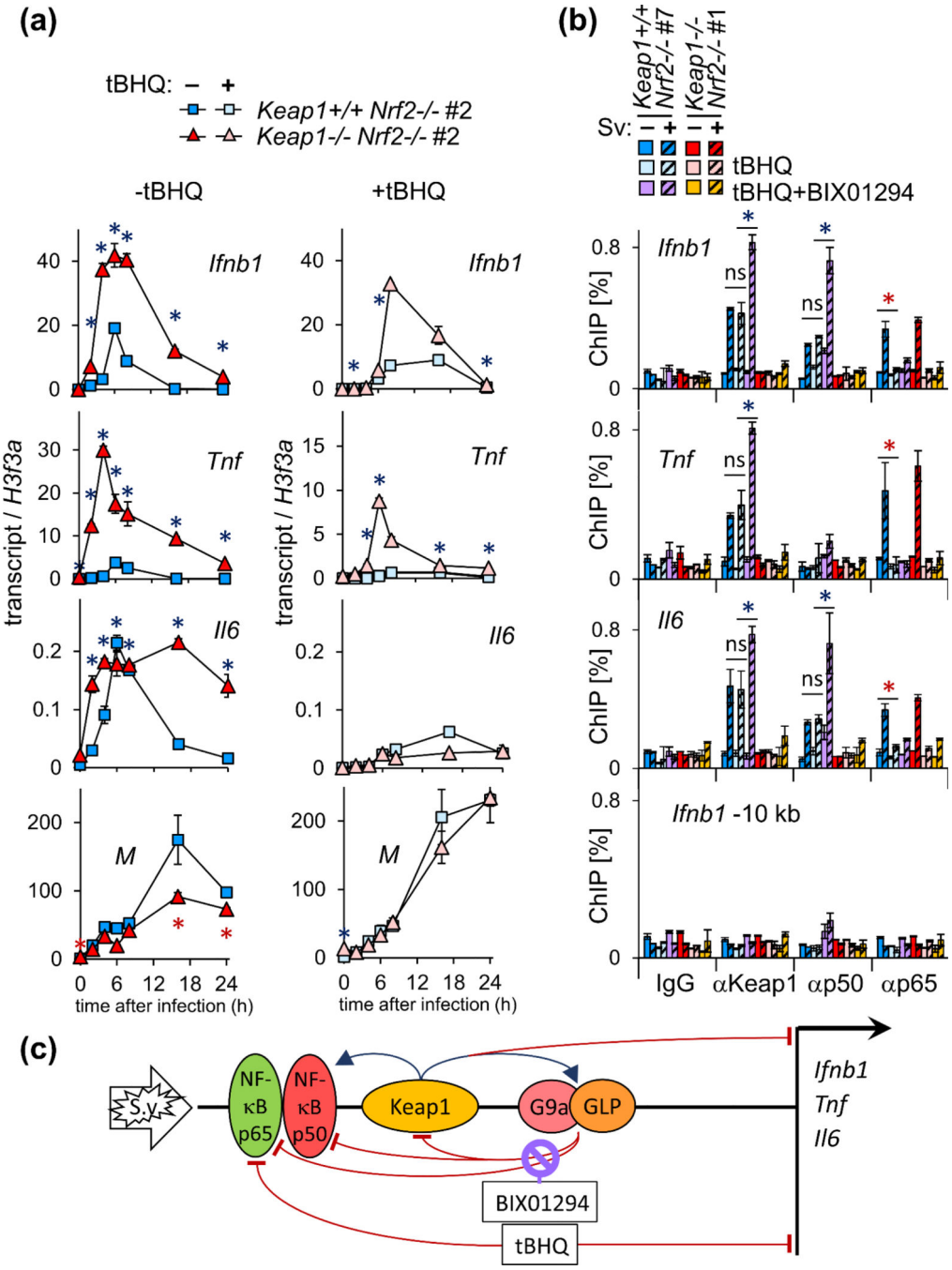

Figure 6. Keap1 and tBHQ reduce virus induced gene transcription through different mechanisms that alter the recruitment of different NFκB subunits.

(a) Keap1 and tBHQ reduce the transcription of virus induced genes independently of each other. MEFs with intact *Keap1* and MEFs with *Keap1−/−* deletions, each with *Nrf2−/−* deletions, were cultured with vehicle (left graphs) or with 50 μM tBHQ (right graphs) for 24 hours before virus infection. The levels of the transcripts indicated in the graphs were measured at the times after virus infection indicated at the bottom. The graphs show the results of a representative experiment in which *Keap1+/+ Nrf2−/−* #2 and *Keap1−/− Nrf2−/−* #2 MEFs were compared. The reproducibility of Keap1 effects on RT-qPCR transcript

signals in MEFs that were cultured with tBHQ or with vehicle were evaluated in two different sets of MEFs by two-factor ANOVA analyses (* $p<0.0005$, blue: increase, red: decrease).

(b) tBHQ inhibits NFκB p65 binding to virus induced genes independently of Keap1. MEFs with intact *Keap1* (cool colors) and MEFs with *Keap1−/−* deletions (warm colors), each with *Nrf2−/−* deletions, were cultured with 50 μM tBHQ, 50 μM tBHQ and 20 μM BIX01294, or vehicle for 24 hours before infection. The levels of Keap1, NFκB p50 and NFκB p65 binding were measured 6 hours after mock (solid bars) or virus (striped bars) infection at the genes indicated in the graphs using the antibodies indicated at the bottom. The graphs show the results of a representative experiment in which *Keap1+/+ Nrf2−/−* #7 and *Keap1−/− Nrf2−/−* #1 MEFs were compared. The reproducibility of tBHQ and BIX01294+tBHQ effects on Keap1, NFκB p50, and NFκB p65 ChIP binding signals were evaluated in two different sets of MEFs by two-factor ANOVA analyses (* $p<0.005$, blue: increase, red: decrease).

(c) The diagram illustrates effects of tBHQ and of BIX01294 on Keap1, NFκB p50, NFκB p65, and H3K9me2 levels, and on transcription at virus induced genes. The blue arrows indicate effects that are required for binding or for deposition. The red arcs and bars indicate effects that inhibit or moderate recruitment, deposition, or transcription.